

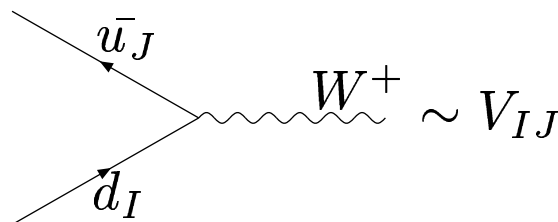
Plan:

- Why should we search the exact informations about Cabbibo-Kobayashi-Maskawa matrix (V_{CKM})?
- V_{CKM} – the only source of CP and flavour violation?
- Classification of SM extensions.
- CP and flavour violation in the Standard Model and its extensions.
- Description of the experimental quantities.
- How to distinguish between models?
- Bounds on new models following from present and future experimental data.
- The examples of the models - 2HDM(II) i MSSM.

The motivation for precise finding the Cabbibo-Kobayashi-Maskawa matrix elements (V_{CKM})

In Standard Model (SM):

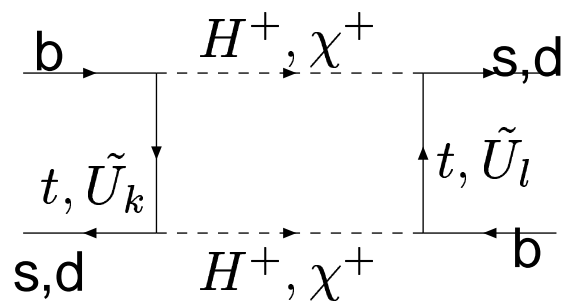
- CP violation is too small to explain $\frac{n_{barion}}{n_{foton}} \sim 10^{-9}$,
- the V_{CKM} matrix describes CP violation and flavour violation,



- this is the only source of CP violation and flavour violation.

How we can classify the extensions of Standard Model with respect to sources CP violation?

1. V_{CKM} matrix is the only one source of CP violation and flavour violation: then the enhancement of CP violated effects arrive by the new particles which give rise to the amplitudes of FCNC (*flavour changing neutral current*) processes.



Example: 2HDM or SUSY models

That effects are especially important in quark b physics $B_{s,d}^0 - \bar{B}_{s,d}^0$, rare decays B mesons, because in vertices stand Yukawa constants of top or bottom (which is large for $\tan \beta \gg 1$).

Processes with b quark are experimentally researched. (e.g.

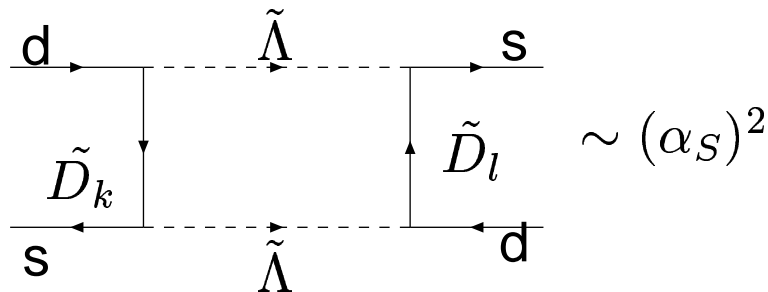
$B_s \rightarrow X_s \gamma$ /CLEO/, $B \rightarrow \Psi K_S$ /BELLE, BaBar/, $B \rightarrow l \bar{l}$ /CLEO/)

How we can classify ...(cont.)

2. New sources (except V_{CKM} matrix) of CP and flavour violation – sfermion mass matrices
 ($u \rightarrow \tilde{U}_L, \tilde{U}_R$)

$$\mathcal{M}_D^2 = \begin{bmatrix} (\mathcal{M}_D^2)_{LL} & (\mathcal{M}_D^2)_{LR} \\ (\mathcal{M}_D^2)_{RL} & (\mathcal{M}_D^2)_{RR} \end{bmatrix}, \quad (1)$$

$(\mathcal{M}_D^2)_{XY}$ $X, Y = L, R \rightarrow 3 \times 3$ matrices.



Flavour changing - in vertices: quark–squark–gluino.

The classification of models with V_{CKM} as the only source of CP violation

One can classify such models on H_{eff} level . It is convenient from phenomenological point of view.

1. The models 'similar to Standard Model' (the MFV model– Minimal Flavour Violation) .

$$H_{eff}^{SM} = C^{VLL} Q^{VLL}$$

In MFV we can factorize in H_{eff} the elements of V_{CKM} . The contribution from t i W^\pm to H_{eff} one can write as:

$$H_{eff}^{\Delta F=2} = \frac{G_F^2 M_W^2}{16\pi^2} \lambda_t^2 \sum_i \tilde{C}_i(\mu) Q_i \quad (2)$$

where

$$\begin{aligned} \lambda_t &= V_{ts}V_{td}^* \text{ dla } K^0 - \bar{K}^0 \\ \lambda_t &= V_{td}V_{tb}^* \text{ dla } B_d^0 - \bar{B}_d^0 \\ \lambda_t &= V_{ts}V_{tb}^* \text{ dla } B_s^0 - \bar{B}_s^0 \end{aligned} \quad (3)$$

\tilde{C}_i are real.

The classification of models ...(cont.)

2. GMFV model (Generalized Minimal Flavour Violation).

Possible contributions from all 8 operators with $\Delta F = 2$

Because V_{CKM} is in models (1.,2.) the only source of CP and flavour violation, in H_{eff} one can factorize the V_{CKM} matrix elements from the Wilson coefficients like in Standard Model.

In SM the contributions to \tilde{C}_i dla $K^0 - \bar{K}^0$, $B_d^0 - \bar{B}_d^0$ i $B_s^0 - \bar{B}_s^0$ are the same (they are given by one function common for all that processes), similar in MFV.

This is no longer true in GMFV.

Rare processes description by H_{eff}

We consider processes with $\Delta F = 2$, because we will use them to find some V_{CKM} matrix elements – V_{td} i V_{ts} (neutral kaons mixing and neutral B^0 mesons mixing).

The examples of the theories above M_W scale: Standard Model(SM), 2-Higgs Doublet Model (2HDM), Minimal Supersymmetric Standard Model (MSSM).

Effective description up to M_W scale by effective Hamiltonian:

$$H_{eff} = \sum_i C_i Q^i. \quad (4)$$

It allow us to take into account QCD correction.

C_i – Wilson coefficients calculated in 'full theory',
 Q^i – local operators built on fermionic fields .

All possible (8) operators dimension 6, which give rise to H_{eff} z $\Delta F = 2$

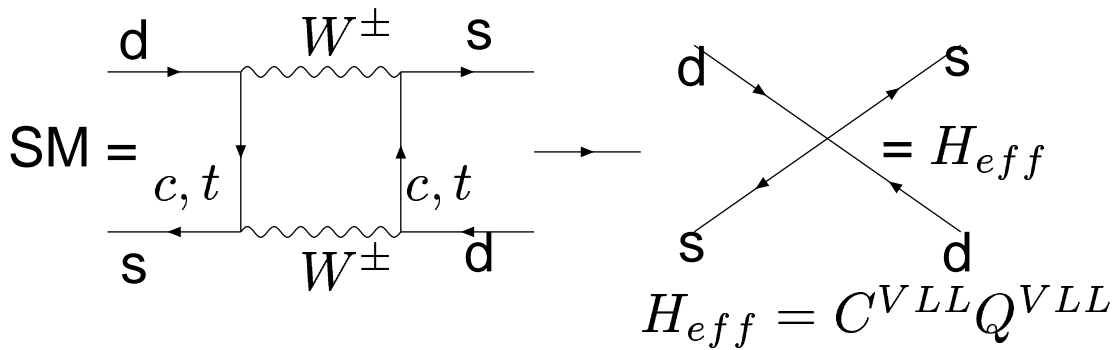
$$\begin{aligned}
 Q^{VLL} &= (\bar{d}_J \gamma_\mu P_L d_I) (\bar{d}_J \gamma^\mu P_L d_I), \\
 Q_1^{LR} &= (\bar{d}_J \gamma_\mu P_L d_I) (\bar{d}_J \gamma^\mu P_R d_I), \\
 Q_2^{LR} &= (\bar{d}_J P_L d_I) (\bar{d}_J P_R d_I), \\
 Q_1^{SLL} &= (\bar{d}_J P_L d_I) (\bar{d}_J P_L d_I), \\
 Q_2^{SLL} &= (\bar{d}_J \sigma_{\mu\nu} P_L d_I) (\bar{d}_J \sigma^{\mu\nu} P_L d_I), \\
 +L &\leftrightarrow R,
 \end{aligned} \tag{5}$$

I, J - flavour indices.

Connection of H_{eff} matrix elements with measurable quantities

$$2\text{Im}\langle \bar{K}^0 | H_{eff} | K^0 \rangle M_{K^0} = \varepsilon_K, \quad (6)$$

$$2\text{Re}\langle \bar{B}^0 | H_{eff} | B^0 \rangle = \Delta M_{d,s}. \quad (7)$$



Contribution to kaons mixing in 'full theory'(SM) and 'effective theory'.

The matrix elements Q^x between hadronic states
(data from lattice calculations):

$$\begin{aligned}\langle \bar{K}^0 | Q^{VLL} | K^0 \rangle &= \frac{8}{3} M_{K^0}^2 f_K^2 \hat{B}_K, \\ \langle \bar{B}^0 | Q^{VLL} | B^0 \rangle &= \frac{8}{3} \hat{B}_{B_d} F_{B_d}^2 M_{B^0}^2\end{aligned}\quad (8)$$

$$\hat{B}_K = 0.85 \pm 0.15,$$

$$\sqrt{\hat{B}_{B_d} F_{B_d}} = 230 \text{ MeV} \pm 40 \text{ MeV},$$

$$\sqrt{\hat{B}_{B_s} F_{B_s}} = 265 \text{ MeV} \pm 40 \text{ MeV}.$$

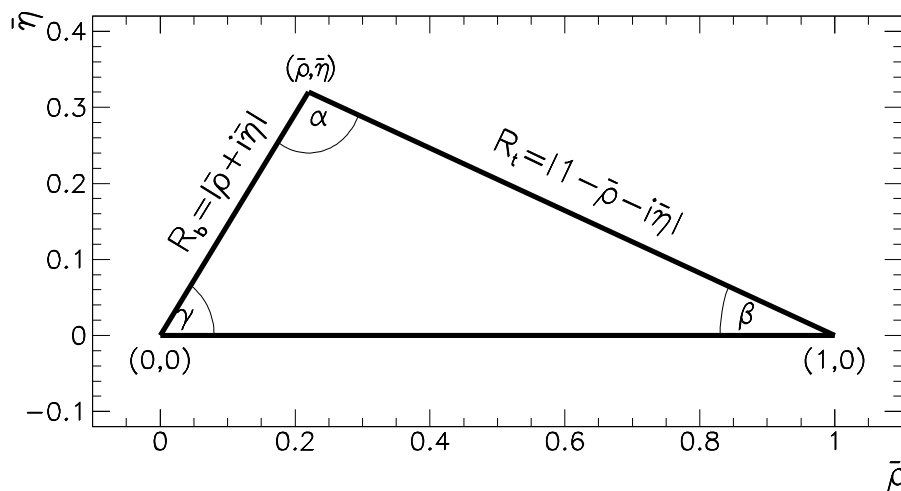
Remark: still large uncertainties!

Wolfenstein parametrization

$$V_{CKM} = \begin{bmatrix} 1 - \lambda^2/2 & \lambda & A\lambda^3(\varrho - i\eta) \\ -\lambda & 1 - \lambda^2/2 & A\lambda^2 \\ A\lambda^3(1 - \varrho - i\eta) & \lambda^2/2 & 1 \end{bmatrix} \quad (9)$$

Wolfenstein parameters: λ , A , $\bar{\varrho}$, $\bar{\eta}$, where A and λ are found from tree-level processes One of orthogonality relation

$$V_{ud}V_{ub}^* + V_{cd}V_{cb}^* + V_{td}V_{tb}^* = 0. \quad (10)$$



Unitarity triangle.

Finding V_{td} from different observables in different models

Experimental quantities: $\Delta M_{d,s}$, ε_K , $\sin 2\beta$.

The formula for $\Delta M_{d,s}$ i ε_K in Standard Model:

- masses differences of neutral mesons B :

$$\Delta M_q = \frac{G_F^2 M_W^2}{6\pi^2} M_{B_q} \eta_B \hat{B}_{B_q} F_{B_q}^2 |V_{tq}|^2 S_0(x_t), \quad q = d, s \quad (11)$$

where $S_0(x_t)$ with $x_t = m_t^2/M_W^2$ is function deriving from diagram (t, W^\pm) (in SM)

$S_0(x_t) \approx 2.38 \pm 0.11$ for $\bar{m}_t(m_t) = (166 \pm 5)$ GeV.

$\Delta M_s/\Delta M_d$ and ΔM_d :

– $\Delta M_d = (0.487 \pm 0.009)/ps$ - uncertainties,

from $\sqrt{\hat{B}_{B_d} F_{B_d}}$

– $\Delta M_s \geq 15.0/ps$ ($\frac{\Delta M_s}{\Delta M_d} \geq 30$),

$$\xi = \frac{\sqrt{\hat{B}_{B_s} F_{B_s}}}{\sqrt{\hat{B}_{B_d} F_{B_d}}} = 1.15 \pm 0.06$$

- we do not know ΔM_s , just upper bound

- ε_K describing CP violating in the neutral kaon system:

$$\bar{\eta} \left[(1 - \bar{\varrho}) A^2 \eta_2 S_0(x_t) + P_c(\varepsilon) \right] A^2 \hat{B}_K = 0.204 \quad (12)$$

Unitarity triangle in GMFV i MFV models

There are 3 processes, in which we will determine V_{CKM} elements – it is convenient to define separate function for each proces:

$$F_{tt}^d = S_0(x_t)[1 + f_d] \quad (\text{for } \varepsilon_K), \quad (13)$$

$$F_{tt}^s = S_0(x_t)[1 + f_s] \quad (\text{for } \Delta M_d),$$

$$F_{tt}^\varepsilon = S_0(x_t)[1 + f_\varepsilon] \quad (\text{for } \Delta M_s)$$

in SM: $f_d = f_s = f_\varepsilon = 0$, $F_{tt}^d = F_{tt}^s = F_{tt}^\varepsilon = S_0(x_t)$

In MFV is $F_{tt}^d = F_{tt}^s = F_{tt}^\varepsilon$.

The formula for ε_K in GMFV:

$$\bar{\eta} [(1 - \bar{\varrho})A^2\eta_2F_{tt}^\varepsilon + P_c(\varepsilon)] A^2\hat{B}_K = 0.204 \quad (14)$$

The formula for ΔM_q in GMFV:

$$\Delta M_q = \frac{G_F^2 M_W^2}{6\pi^2} M_{B_q} \eta_B \hat{B}_{B_q} F_{B_q}^2 |V_{tq}|^2 F_{tt}^q, \quad q = d, s \quad (15)$$

As in SM, in GMFV we can determine R_t in 2 ways:
from ΔM_d and $\Delta M_d/\Delta M_s$:

$$R_t = 1.084 \frac{R_0}{A} \frac{1}{\sqrt{F_{tt}^d}} \quad (16)$$

$$R_0 \equiv \sqrt{\frac{\Delta M_d}{0.487/\text{ps}}} \left[\frac{230 \text{ MeV}}{\sqrt{\hat{B}_{B_d} F_{B_d}}} \right] \sqrt{\frac{0.55}{\eta_B}}$$

and

$$R_t = 0.819 \xi \sqrt{\frac{\Delta M_d}{0.487/\text{ps}}} \sqrt{\frac{15/\text{ps}}{\Delta M_s}} \sqrt{R_{sd}}, \quad (17)$$

$$R_{sd} = \frac{1 + f_s}{1 + f_d} \quad (18)$$

In MFV $R_{sd} = 1$ (R_t found from $\Delta M_d/\Delta M_s$ does not depend on parameters of model).

How to distinguish between GMFV and MFV models?

The question is how to check experimentally, if MFV's are sufficient?:

- if the experimental value of $\sin 2\beta$ is small (smaller than 0.42) then MFV models are excluded.

In the MFV models there exists an *absolute* lower bound on $\sin 2\beta$ that follows from the interplay of ΔM_d and ε_K and depends mainly on V_{cb} , V_{ub} and the non-perturbative parameters \hat{B}_K , $F_{B_d} \sqrt{\hat{B}_{B_d}}$ entering the analysis of the unitarity triangle. Lower bound on $\sin 2\beta$ obtained by scanning independently all relevant input parameters reads $(\sin 2\beta)_{\min} = 0.42$,

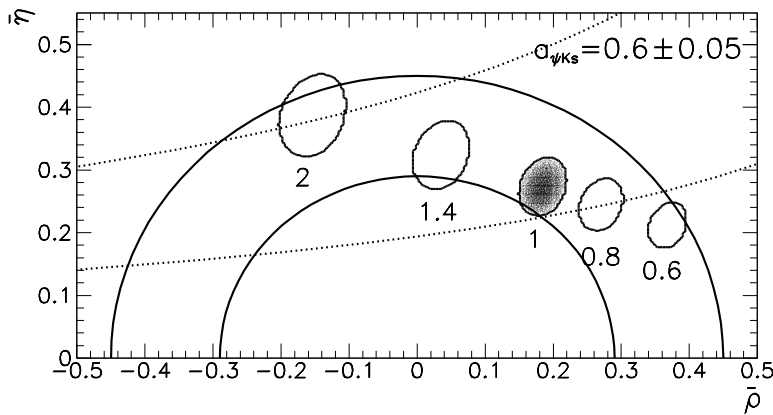
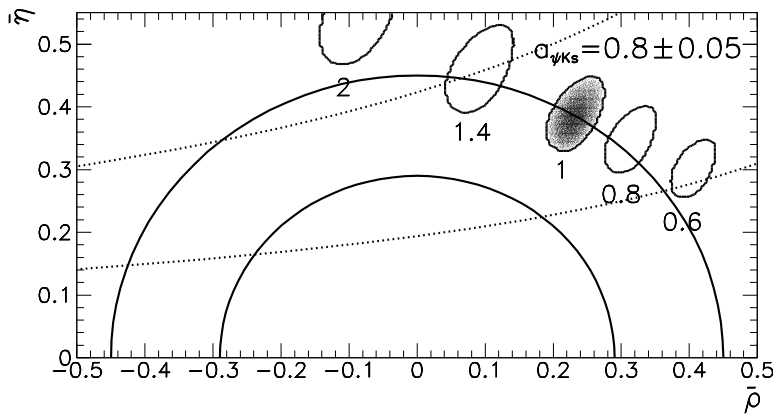
- if the experimental value $\sin 2\beta$ will be above this bound, then we analyze the correlations between $\Delta M_d / \Delta M_s$, $\sin 2\beta$ and another quantities like ε_K or γ .

- 'strategy A': if we know experimental value of $\Delta M_d/\Delta M_s$, then we know R_t for any R_{sd} - so we can find $\sin 2\beta$ (and we can compare with experimental results):

$$R_t \sim \frac{1}{\sqrt{\Delta M_s/\Delta M_d}} \sqrt{R_{sd}} \quad (19)$$

$$R_t, R_b \rightarrow \sin 2\beta$$

- 'strategy B': if we know experimental value for $\Delta M_d/\Delta M_s$ and $\sin 2\beta$, we can find the value of the γ angle (from $B \rightarrow \pi K$)



Ranges of $(\bar{\rho}, \bar{\eta})$ allowed in 1σ for $\Delta M_s = (18.0 \pm 0.5)/ps$, three values of $a_{\psi K_S}$ and different values of R_{sd} (marked in the figures). Black spots correspond to $R_{sd} = 1$. Dotted lines show the constraint from ϵ_K , for $1 + f_\epsilon = 1$.

How to find bounds on $F_{tt}^{d,s,\varepsilon}$ function in concrete model?

- from fitting the formula (15) to the measured (in the near future) value of ΔM_s . This determines $1 + f_s$ (or F_{tt}^s):

$$1 + f_s = 0.80 \left[\frac{2.38}{S_0(x_t)} \right] \left[\frac{265 \text{ MeV}}{\sqrt{\hat{B}_{B_s} F_{B_s}}} \right]^2 \left[\frac{0.55}{\eta_B} \right] \left[\frac{0.041}{|V_{ts}|} \right]^2 \left[\frac{\Delta M_s}{15/\text{ps}} \right] \quad (20)$$

scanning over uncertainties gives

$$0.52 \left[\frac{\Delta M_s}{15/\text{ps}} \right] < 1 + f_s < 1.29 \left[\frac{\Delta M_s}{15/\text{ps}} \right] \quad (21)$$

(at present this gives $1 + f_s > 0.52$)

next, there are bounds on R_t coming from unitarity of V_{CKM} matrix

$$1 - R_b < R_t < 1 + R_b \quad (22)$$

- if we make use on experimental result on ε_K , we can corelate F_{tt}^ε with R_{sd} .

Allowed ranges of R_{sd} and $1 + f_\varepsilon$.

- $\frac{\Delta M_s}{\Delta M_d}$, ε and R_b allow the region delimited by the dashed lines.
- Regions between the solid lines are allowed by ΔM_d , ε and $\sin 2\beta = 0.4$ (panel a) and $\sin 2\beta = 0.8$ (panel b).
- Dotted regions are allowed by $\frac{\Delta M_s}{\Delta M_d}$, ε and R_b for $\sin 2\beta = 0.8$ and 0.79 ± 0.10 in panels a) and b), respectively.

The examples of GMFV models

1. 2HDM(II) with large $\tan \beta$

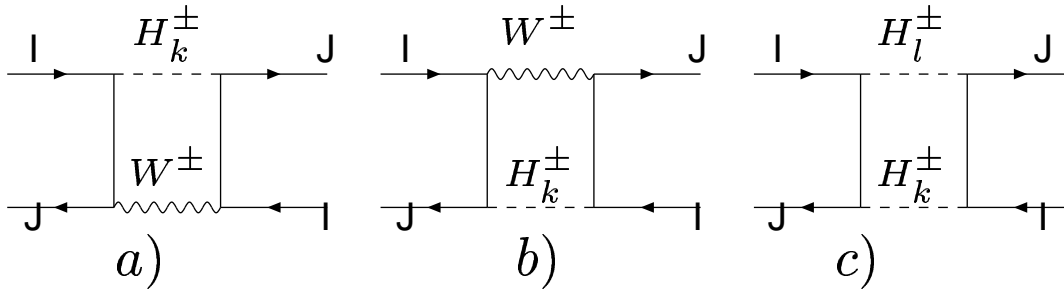
tree-level coupling of charged Higgs scalar ($H_k^+ \equiv (H^+, G^+)$) to quarks:

$$L_{\text{int}} = H_k^+ \bar{u}_A V_{AI} (a_L^{AIk} P_L + a_R^{AIk} P_R) d_I + \text{H.c.} \quad (23)$$

where

$$a_L^{AIk} = \frac{e}{\sqrt{2}s_W} \frac{m_{u_A}}{M_W} \times \begin{cases} \cot \bar{\beta} & \text{for } k = 1 \\ 1 & \text{for } k = 2 \end{cases} \quad (24)$$

$$a_R^{AIk} = \frac{e}{\sqrt{2}s_W} \frac{m_{d_I}}{M_W} \times \begin{cases} \tan \bar{\beta} & \text{for } k = 1 \\ -1 & \text{for } k = 2 \end{cases} \quad (25)$$



Box diagrams in extended Higgs sector

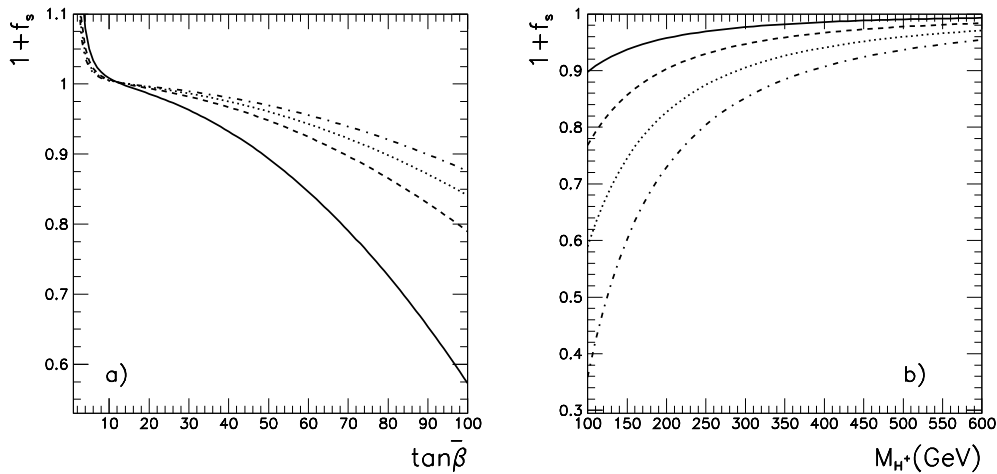
dominant contributions to Wilson coefficients:
 diagram with $W^\pm H^\mp$:

$$\delta^{(+)} C_2^{LR} \sim -\frac{8 m_{d_I} m_{d_J}}{3 m_t^2} \tan^2 \bar{\beta}$$

diagram with $H^\pm H^\mp$:

$$\delta^{(+)} C_2^{LR} \sim -\frac{4 m_{d_I} m_{d_J}}{3 M_W^2} \tan^2 \bar{\beta} \tag{26}$$

It is clear that for large $\tan \bar{\beta}$ the biggest contribution appears in $\delta^{(+)} C_2^{LR}$. It is of the opposite sign than the contribution of the tW^\pm box diagram and can be significant only for the $\bar{B}_s^0 - B_s^0$ (similar contributions to $\delta^{(+)} C_2^{LR}$ for $\bar{B}_d^0 - B_d^0$ and $\bar{K}^0 - K^0$ transitions are suppressed by factors m_d/m_s and m_d/m_b , respectively).



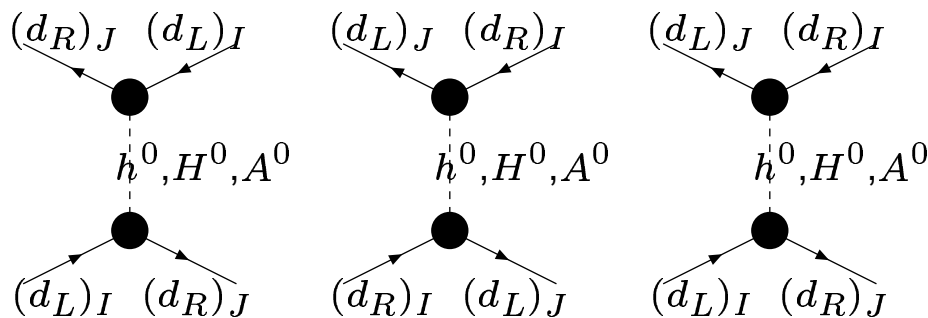
$1 + f_s$ in the 2HDM(II): a) as a function of $\tan\beta$ for $M_{H^+} =$ (from below) 150, 250, 300 and 350 GeV and b) as a function of M_{H^+} for $\tan\beta =$ (from above) 40, 60, 80 and 100.

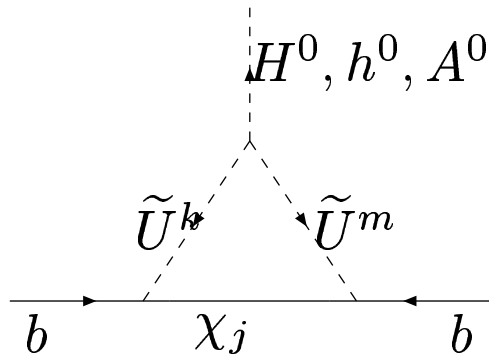
The computation of the $b \rightarrow s\gamma$ rate together with the experimental result for this process

$BR(B \rightarrow X_s\gamma) = (3.03 \pm 0.40 \pm 0.26) \times 10^{-4}$ set the bound $M_{H^+} \gtrsim 350$ GeV. This means that in the 2HDM(II) for the still allowed range of charged Higgs boson masses the decrease of $1 + f_s$ can be very small. Consequently, the SM analysis of the unitarity triangle based on ε , ΔM_d and ΔM_s is practically unchanged in the 2HDM(II) for large $\tan\beta \lesssim 50$.

2. MSSM with large $\tan\beta$, heavy sparticles and light Higgs sector

- in the limit of heavy sparticles (which is practically realized already for $M_{\text{sparticles}} \gtrsim 500$ GeV) the one loop diagrams involving charginos and stops are negligible.
- one loop diagrams with charged Higgs and top quark can give large ($\sim \tan^2\beta$) contributions (the bound on M_{H^+} from $b \rightarrow s\gamma$ is much weaker)
- two loop corrections, deriving from one loop corrections to down quarks with neutral Higgs couplings (double penguin diagram), can be very large ($\sim \tan^4\beta$)





One-loop correction to the $\bar{b}b$ -neutral Higgs vertex in MSSM (contribution charginos and stops in loop), proportional to $\tan \beta^2$.
 Such kind of effects does not vanish with very heavy sparticles.

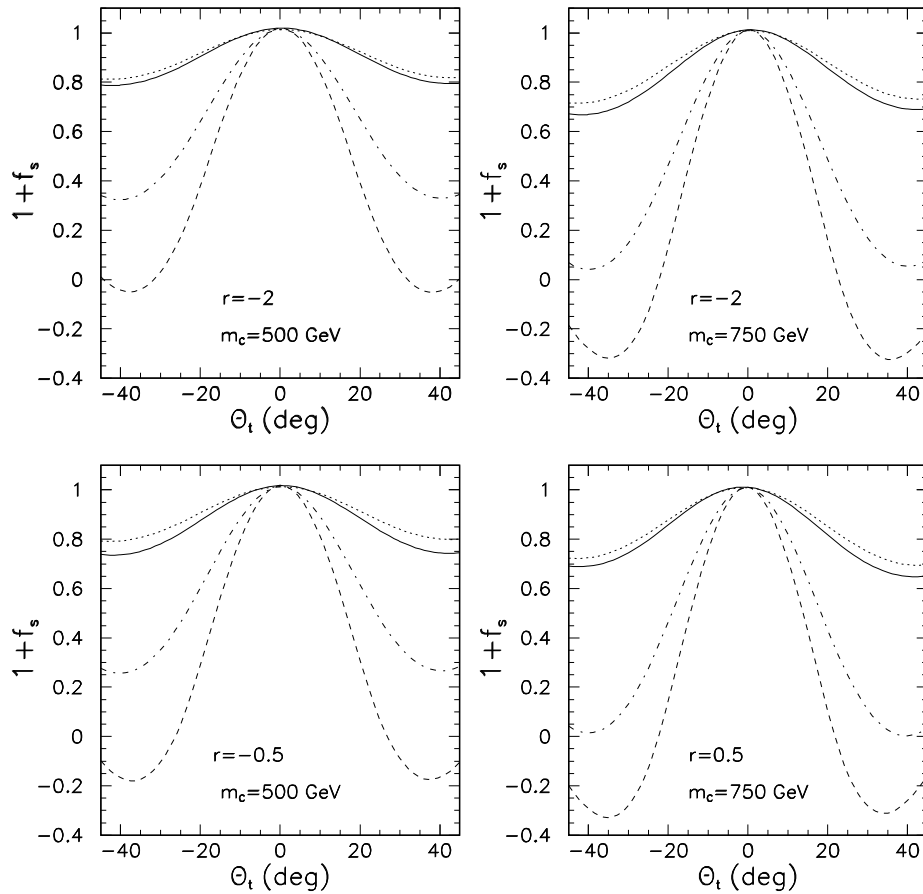
Identical diagrams give rise to $B \rightarrow \bar{l}l$ amplitude, so very strong effects which was expected in that proces can be partially limited by neutral B meson mixing.

The contributions of diagrams (from previous figure) to Wilson coefficients:

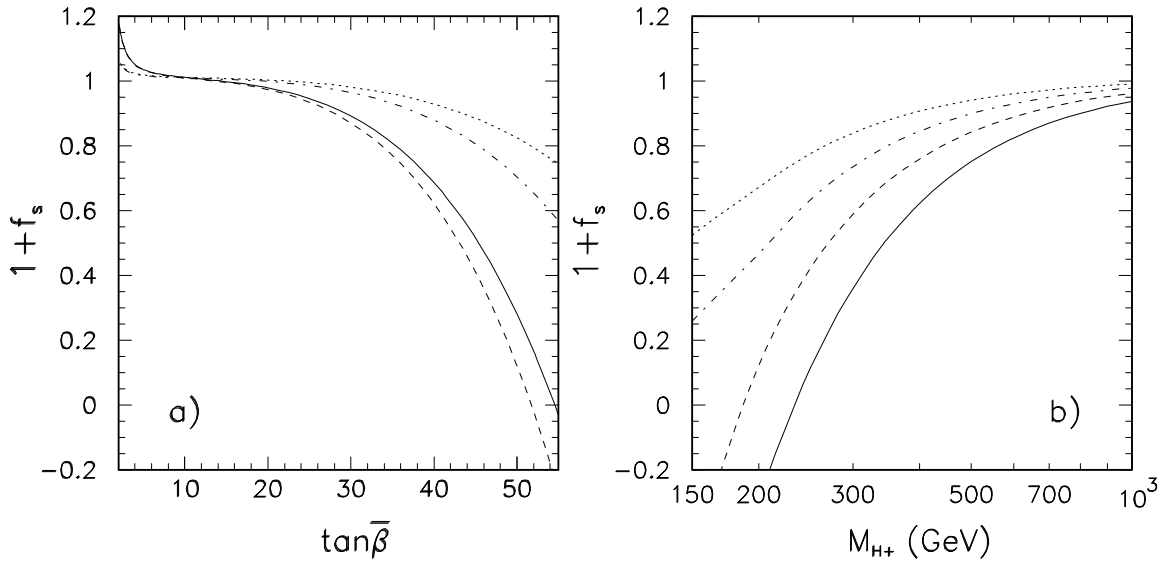
$$\begin{aligned}
 \delta^{(0)} C_1^{\text{SLL}} &= -\frac{\alpha_{EM}}{4\pi s_W^2} \frac{m_t^4}{M_W^4} m_{d_J}^2 X_{tC}^2 \tan^4 \bar{\beta} \mathcal{F}_- \\
 \delta^{(0)} C_1^{\text{SRR}} &= -\frac{\alpha_{EM}}{4\pi s_W^2} \frac{m_t^4}{M_W^4} m_{d_I}^2 X_{tC}^2 \tan^4 \bar{\beta} \mathcal{F}_- \quad (27) \\
 \delta^{(0)} C_2^{\text{LR}} &= -\frac{\alpha_{EM}}{2\pi s_W^2} \frac{m_t^4}{M_W^4} m_{d_J} m_{d_I} X_{tC}^2 \tan^4 \bar{\beta} \mathcal{F}_+ .
 \end{aligned}$$

where $X_{tC} = \sum_{j=1}^2 Z_+^{2j} Z_-^{2j} \frac{A_t}{m_{C_j}} H_2(x_1^{t/C_j}, x_2^{t/C_j})$,
 $x_i^{t/C_j} = M_{\tilde{t}_i}^2 / m_{C_j}^2$, $i = 1, 2, j = 1, 2$,

$$\mathcal{F}_{\mp} \equiv \left[\frac{\cos^2 \bar{\alpha}}{M_H^2} + \frac{\sin^2 \bar{\alpha}}{M_h^2} \mp \frac{\sin^2 \bar{\beta}}{M_A^2} \right] \quad (28)$$



$1 + f_s$ in the MSSM as a function of the mixing angle of the top squarks for different lighter chargino masses and compositions ($r \equiv M_2/\mu$). Solid, dashed, dotted and dot-dashed lines correspond to stop masses (in GeV) (500,650), (500,850), (700,850) and (700,1000), respectively.



$1 + f_s$ in the MSSM for lighter chargino mass 750 GeV, $r \equiv M_2/\mu = -0.5$ and stop masses (in GeV) (500,850), (700,1000), (500,850) and (600,1100) (solid, dashed, dotted and dot-dashed lines, respectively) as a function of a) $\tan \bar{\beta}$ and b) M_{H^+} . In panel a) solid and dashed (dotted and dot-dashed) lines correspond to $M_{H^+} = 200$ (600) GeV, and in panel a) solid and dashed (dotted and dot-dashed) lines correspond to $\tan \bar{\beta} = 50$ (35).

Conclusions:

- Classification of SM extensions .
- Analysis of the role of new dimension six four-fermion $|\Delta F| = 2$ operators in models with minimal flavour violation (MFV and GMFV).
- Formulae for the mass differences ΔM_s , ΔM_d and the CP violation parameter ε (parametrization by three real functions F_{tt}^s , F_{tt}^d and F_{tt}^ε , respectively).
- We have proposed a few simple strategies involving the ratio $\Delta M_s / \Delta M_d$, $\sin 2\beta$ and the angle γ that allow to search for the effects of the new operators.
- The present experimental and theoretical uncertainties allow for sizable contributions of new operators to $\Delta M_{s,d}$ and ε .
- As an example we have analyzed the role of new operators in the MSSM with large

$\tan \bar{\beta} = v_2/v_1$ in the limit of heavy sparticles,
investigating in particular the impact of the
extended Higgs sector on the unitarity triangle.
The largest effects of new contributions for large
 $\tan \bar{\beta}$ are seen in ΔM_s .